

Why we need a standardized state of health definition for electric vehicle battery packs – a proposal for energy- and capacity-based metrics

Philip Bilfinger^{1*}, Markus Schreiber¹, Philipp Rosner¹,
Kareem Abo Gamra¹, Jan Schöberl¹, Cristina Grosu¹,
Markus Lienkamp¹

¹Institute of Automotive Technology (FTM), Technical University of Munich (TUM), Boltzmannstr. 15, Garching, 85748, Bavaria, Germany.

*Corresponding author(s). E-mail(s): philip.bilfinger@tum.de;
Contributing authors: markus.schreiber@tum.de; philipp.rosner@tum.de;
kareem.abo-gamra@tum.de; jan.schoeberl@tum.de;
cristina.grosu@tum.de; lienkamp@tum.de;

Abstract

Range and performance are key customer-relevant properties of electric vehicles. Both degrade over time due to battery aging, thus impacting business decisions throughout a vehicle's lifecycle, such as efficient utilization and asset valuation. For practical assessment, aging is often simplified into a single figure of merit – the state of health – typically defined by the battery pack's remaining capacity or energy. However, no standardized method for measuring the state of health at the vehicle level has been established, leaving both academia and industry without a clear consensus. Ultimately, standardization is crucial to increase transparency and build confidence in the long-term reliability of electric vehicles' battery packs. In this article, we propose a standard measurement procedure for assessing the capacity- and energy-based state of health, leveraging onboard charging to enable reproducibility and scalability. Additionally, we demonstrate how differential voltage analysis can provide deeper insights into battery aging at the vehicle level.

Keywords: Battery aging, Battery pack diagnostics, Differential voltage analysis, Electric vehicle, Lithium-ion battery, State of health

Introduction

Electric vehicles (EVs) have emerged as the breakthrough solution to decarbonize and electrify the transportation sector, capable of significantly reducing greenhouse gas emissions [1]. Enablers for the acceptance of electric mobility and exponential growth in EV sales are advancements and innovations in their battery packs, which are currently mostly assembled with lithium-ion batteries (LIBs) [2]. These battery packs must satisfy the customer’s required achievable range and power capabilities, embodying central properties for purchasing an EV [3]. However, these capabilities degrade throughout the EV’s usage life due to a complex and coupled interplay of reversible and irreversible aging mechanisms [4]. Typically, battery aging is generally expressed by means of the state of health (SOH) that aggregates degradation in the remaining capacity or energy, expressed as a scalar value in reference to pristine conditions [5]. On the vehicle level, this offers a simple approach directly correlating to the remaining achievable range of an EV [6]. However, to our knowledge, neither industry nor academia has a consensus on a vehicle-level SOH definition or a standard procedure for its measurement, lacking standardization and a common understanding of how aging shall be characterized for EVs. Furthermore, only considering the overall capacity- or energy loss superficially reflects battery aging, i.e., EVs with the same SOH might have degraded through different aging mechanisms [7].

Hence, with increasing efforts to establish a holistic and circular battery ecosystem, it is vital to precisely express battery degradation to achieve an accurate SOH representation [8]. This allows stakeholders along the entire EV value chain to operate the battery within ideal parameters and make informed decisions regarding maintenance, use in second-life applications, or recycling, thus maximizing resource efficiency and reducing costs [9]. Furthermore, an accurate depiction in the SOH provides transparency regarding insurance premiums or liability decisions in warranty claims [10]. It also lays the foundation for assessing the residual value of secondhand vehicles [11]. In summary, a transparent, reproducible standard measurement is necessary for a vehicle-level SOH definition that covers the overall capacity/energy loss and enables deeper insights into the degradation condition of the battery pack.

This article emphasizes the importance of vehicle-level SOH standardization and proposes a transparent and reproducible standard measurement for capacity- and energy-based metrics derived from electrochemical properties of LIBs and designed for in-vehicle utilization. The overall aim is to close the gap between the necessity of a vehicle-level SOH definition and the uncertainty of its determination, which is necessary for accepting battery electric vehicles as a suitable long-term alternative to conventional vehicles.

Results

Regulation, standardization, and the EU battery passport

The importance of SOH standardization has reached the political arena as numerous political institutions have imposed and regularly expanded regulations to guarantee sustainability, safety, and quality standards for products containing batteries, with recent extensions to EVs [12]. Most notable is European Union (EU) Regulation 2023/1542, making a digital battery passport mandatory for new EVs entering service by 2027 [13]. The overall goal is to define technical standards, among which the SOH is explicitly named as an essential performance metric of batteries, aiming at a more sustainable battery value chain. However, its articles concerning the SOH lack technical detail and merely state that it must be given as an energy-based value for electric vehicles, named the state of certified energy (SOCE). Additionally, a rated capacity must be given in the vehicle registration documents, which is not explicitly appointed as a reference for the SOH but can serve as one. Ultimately, the regulation misses a definition of standard measurement and reference for obtaining the SOH or SOCE, which substantially impacts the values obtained. This has also been criticized by the battery pass consortium [14], a publicly funded initiative uniting strategic partners in the field of EVs, which demands regulatory clarity.

Solely United Nations (UN) Global Technical Regulation No. 22 [15], incorporated into the EURO 7 [16] to regulate emissions and battery durability of motor vehicles, addresses the necessity and challenges for vehicle-level health metrics. The regulation advocates for "in-use verification" via the tailored EV driving cycle Worldwide harmonized Light Duty Test Cycle (WLTC) through which the SOCE and state of certified range (SOCR) are determined, but not the remaining capacity, which is, however, necessary for the previously mentioned EU regulation.

International standards are equally unsuited, e.g., ISO 12405-4 [17] vaguely proposes standard (dis)charging cycles for battery packs of EVs relying on the battery "supplier's recommendations," which are not publicly available.

The goal of SOH standardization for EVs is definite from a political point of view. However, the labyrinth of regulation and standardization lacks a clear definition of what constitutes a vehicle level SOH, to which reference it is based, and how it shall be measured.

Viable approaches for a vehicle-level battery state of health standard measurement

The general methodologies for defining a standard measurement for an EV's SOH are reviewed in this section and can be classified into model-based and measurement-based approaches.

Model-based approaches estimate the SOH, e.g., through electrochemical or equivalent circuit models, but inherit model inaccuracies and are either unsuitable for online application or imprecise [18]. The SOH read directly from the vehicle's battery management system (BMS) is estimated by such models [5]. However, this SOH is supplied

by the original equipment manufacturer (OEM), which can have an incentive to manipulation so that it does not necessarily coincide with actual battery aging. Therefore, exclusive reliance on model-based approaches is not recommended.

Measurement-based approaches actively stress the EV's battery pack either by discharging or charging, which is further discussed in terms of their suitability for standard measurement and data processing, with an overview in Figure 1.

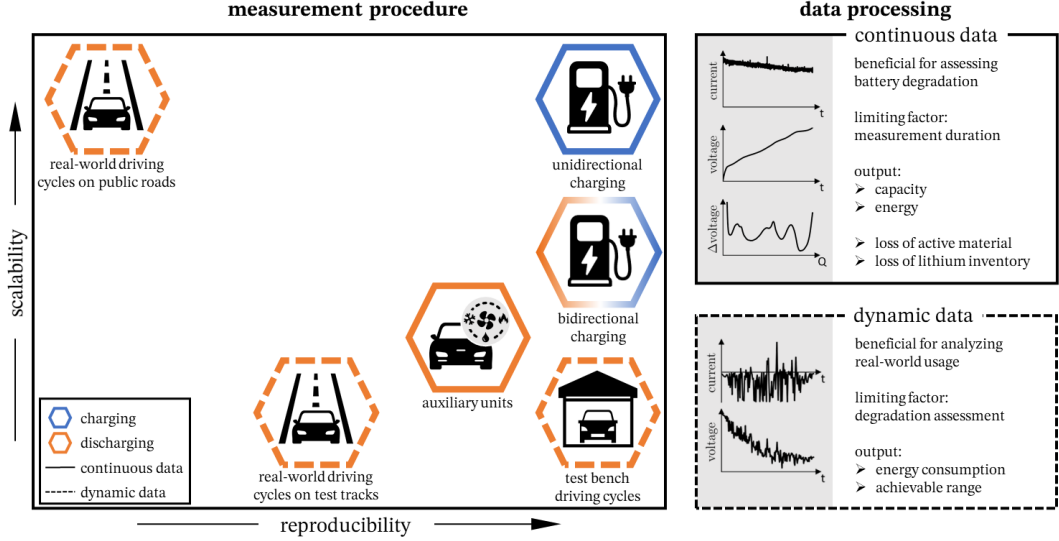


Fig. 1: Qualitative evaluation of viable SOH standard measurements at the vehicle level, focusing on scalability for in-vehicle utilization and reproducibility of the measurement procedure. A standard measurement method based on unidirectional charging satisfies both criteria. The data obtained from EV measurements can either be continuous or dynamic. The former is suited for deeper battery degradation analysis, and the latter for real-world consumption and range analysis.

Discharging the battery pack during driving cycles mimics an EV's actual operation and use case, which can be performed on test benches (e.g., chassis dynamometer) or on the road. The former ensures reproducibility but is cumbersome, time-consuming, and expensive, impairing scalability. Real-world driving profiles on the road are an application advantage but not reproducible due to fluctuating external influences. Furthermore, due to the dynamic loads, insights into the batteries' behavior and degradation states are difficult to obtain. Therefore, driving profiles, neither on a test bench nor on (public) roads, are suitable as a standard measurement for the SOH but are important for actual real-world energy consumption and range estimations of EVs.

Continuous discharging of the battery by auxiliary units is possible for a reproducible measurement but is time-consuming and less applicable in operation as energy is wasted through heat dissipation, and recharging is necessary for the following use.

A bidirectional charging standard can provide an opportunity for a controlled discharging procedure and automated recharging without significant energy loss, but it has yet to be widely adopted [19].

A scalable and reproducible approach relies on onboard charging, as stressing the battery pack takes place in a controlled manner defined by standardized protocols (e.g., ISO 15118 or IEC 61851). Hereby, thermodynamic changes in the voltage signal can be captured for further degradation assessment, e.g., by differential voltage (DV) analysis, which can provide detailed information on where the overall capacity/energy loss occurs [20]. The measurement can conveniently be integrated into vehicle operation to monitor the SOH throughout the vehicle’s lifetime, as EVs must regularly be charged, and the availability of chargers has increased throughout the years, especially wallboxes for homeowners [21]. Hereby, using alternating current (AC) or direct current (DC) chargers is arbitrary when sampling data from the EV’s BMS, as the charging power is ultimately transformed into the battery pack’s DC system. A benefit of DC charging is the capability of charger-side data acquisition due to necessary standardized communication norms (e.g., ISO 15118), where the battery pack’s voltage and current values are periodically transmitted to the charger’s backend. Given these advantages, onboard charging is best suited for developing a SOH standard measurement for EV battery packs.

A standard charging measurement proposal

Any standard measurement must be unambiguously defined for transparency and reproducibility. For a standard charging measurement, shown in Figure 2a for a Volkswagen (VW) ID.3, this implies fixed conditions for the charging procedure, including the charging rate and cut-off constraints, the ambient temperature, and the preparation setup [22].

The maximum charging rate must meet a trade-off between the overall measurement duration and the containment of overpotentials that stem from ohmic and kinetic resistances in the batteries [23]. The latter limits the transferable capacity/energy, which are, however, the quantities of interest [22]. Therefore, a measurement duration of at least $t = 15$ h is proposed to contain the influence of overpotentials. The measurement time seems lengthy but yields the most accurate results, which is further discussed in Section 1. The maximum charging power can be determined for each EV by the $E - rate$, which is the inverse of the charging time t normalized by the battery pack’s net energy, as given in Equation 1.

$$E - rate = \frac{P_{max}}{E_N} < \frac{1}{t} \Rightarrow P_{max} < \frac{1}{t} \cdot E_N \quad (1)$$

With typical battery pack energies up to 120 kWh [24], this results in a maximum charging power of 8 kW, which is below typical wallbox powers in the EU of 11 kW enabling simple utilization. For charging, we propose a constant power (CP) protocol, as it is common for EV charging due to energy conservation with the grid.

Furthermore, the minimum measuring window, i.e., the cut-off conditions, must be defined either by a state of charge (SOC) window or voltage range. Fixing a voltage

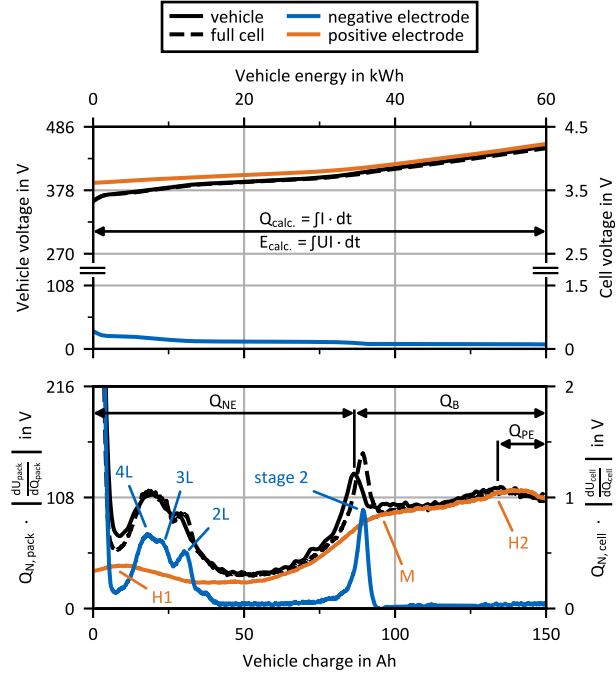


Fig. 2: Charging measurement of a VW ID.3 following the proposed standard measurement. a) Full and half-cell laboratory measurements from a VW ID.3 pouch cell are aligned to the vehicle’s voltage and capacity data, showing the transferability of cell-specific characteristics like the potential contribution of the positive and negative electrodes during (de)lithiation. b) DV curves are calculated from the derivation of the voltage signal and enable deeper analysis of the battery’s electrochemical condition. Changes in the characteristic capacities Q_{NE} , Q_{PE} , and Q_B throughout aging enable the calculation of degradation modes to determine loss of active material (LAM) at the negative electrode (NE), positive electrode (PE), and loss of lithium inventory (LLI) [55]. DV analysis can also be utilized on the vehicle level, but limitations are to be considered, e.g., cell-to-cell variations in the pack (see differences at stage 2) [20].

range is unambiguous, as the voltage is a directly measurable quantity, unlike the SOC, which can underlie estimation errors and is prone to manipulation [25]. However, the voltage is less accessible and currently must be reverse-engineered from controller area network (CAN) data so that simple access to the voltage must be granted, e.g., through the onboard diagnosis (OBD)-II interface [26]. Nonetheless, a fixed pack-level voltage window should be used for reproducible and comparable measurements, which must be declared in the vehicle’s registration documents. The voltage range should hereby be as broad as necessary to capture characteristic changes in the voltage signature but as narrow as possible with the cut-off voltages reachable in the typical operation window of an EV to ensure applicability. Some authors seek applicability by

correcting a partial charging measurement with the SOC range of the measurement, i.e., $Q = Q_{\text{partial}}/\Delta\text{SOC}$ [27, 28]. However, a direct measurement without the estimated SOC is more accurate.

Additionally, a rest period prior to the measurement is recommended to allow potential gradients within the battery pack to decay exponentially, with the required duration depending on the excitation prior to the measurement [29]. A practical rule of thumb can be derived from Fernando et al. [30] that consider the voltage settled when its rate of change falls below $1 \text{ mV s}^{-1} \cdot n_s$, where n_s is the number of serially connected cells, or when the variation is smaller than the voltage sensor's resolution. For example, a 30-minute rest period was sufficient in this study to achieve a stable voltage. Generally, the necessary resting time will increase when the battery pack is stressed with higher loads prior to the measurement or at lower temperatures [30]. Furthermore, the relaxed battery pack should settle below the predefined lower voltage threshold so that the defined voltage window is captured entirely.

Lastly, the behavior of LIBs is strongly influenced by the temperature, so cold or hot ambient conditions shall be avoided for reproducibility [31]. Hence, spatially measured temperatures within the battery pack should lie at room temperature of 20°C in a window of $\pm 5^\circ\text{C}$ before the measurement, and charging in an air-conditioned workshop or garage is recommended [32]. Naturally, the battery's temperature increases during the charging measurement, which can additionally be monitored to detect hot spots within the pack. However, excessive temperatures are typically contained by an EV's thermal management system, e.g., the temperatures of the specimens under test never exceeded 30°C after the termination of the charging session [26].

The battery pack's capacity Q_{calc} and energy E_{calc} are then calculated by time integration between the lower cut-off voltage U_{low} until the upper cut-off voltage U_{high} is reached by

$$Q_{\text{calc}} = \int_{t_{U_{\text{low}}}}^{t_{U_{\text{high}}}} I \, dt \quad (2)$$

$$E_{\text{calc}} = \int_{t_{U_{\text{low}}}}^{t_{U_{\text{high}}}} P \, dt = \int_{t_{U_{\text{low}}}}^{t_{U_{\text{high}}}} U I \, dt \approx U_n \cdot Q_{\text{calc}}. \quad (3)$$

The energy E_{calc} is application-oriented, reflecting the usable energy in power-coupled systems, e.g., with inverters and electric motors, and characterizes aging more closely to the customer's perception, specifically the vehicle's range at a given energy consumption. In contrast, the capacity Q_{calc} plainly accounts for the charge transferred between the electrodes, independent of the voltage and the effect of overpotentials. Therefore, capacity provides a consistent basis for comparing changes in electrode capacities to determine underlying degradation modes [33].

For simplicity, some authors calculate the energy E_{calc} by multiplying the calculated capacity by the nominal voltage U_n of the battery pack, which must be available in the vehicle's registration documents, but only suits as an approximation [34].

Regularly performing this standard measurement and referencing the measured capacity and energy to the nominal values Q_N/E_N results in the capacity-based SOH_Q and energy-based SOH_E by

$$SOH_Q = \frac{Q_{calc}}{Q_N} \quad (4)$$

$$SOH_E = \frac{E_{calc}}{E_N} \quad (5)$$

If available, the calculated capacity and energy can be referenced to an initial value Q_0/E_0 reflecting an EV's individual $SOH_{Q/E}$.

Battery pack diagnostics with differential voltage analysis

The proposed 15-hour measurement is suited for vehicle-level DV analysis, as analyzed by Schmitt et al. [35], enabling deeper insights into battery degradation through the identification of chemistry-specific characteristics. Nonetheless, lower charging powers are favorable with the cost of a longer measurement, as features for DV analysis tend to be more pronounced [36]. Thus, the measurements in this article were conducted at approx. 2 kW. In DV analysis, local maxima, shown in Figure 2b for a nickel cobalt manganese oxide (NMC)/graphite chemistry, indicate lithiation stages of the LIB, which can mostly be unambiguously assigned to either the positive electrode (PE) or negative electrode (NE) [37]. Tracking these maxima enables the calculation of the electrode capacities $Q_{NE/PE}$ and their balancing Q_B . These capacities change with aging, from which the degradation modes loss of active material (LAM) at the electrodes and loss of lithium inventory (LLI) can be determined, and aging can be further dissected [38]. Note that available characteristic features depend on the cell chemistry, so the degradation assessment must be tailored to the underlying battery pack [7]. Nonetheless, the general methodology is transferable, as shown by a previous publication, where vehicles with different battery pack setups are compared [20]. Also, other aging diagnostic methods, such as incremental capacity analysis (ICA), benefit from the proposed charging procedure and can be utilized on the vehicle level [11]. Nonetheless, it is clear that battery diagnosis, e.g., through DV analysis, is not necessary for obtaining a battery pack's SOH but rather enables test facilities for a more profound analysis of the battery's aging state.

Application of the proposed method

The application and universality of the proposed method is shown in Figure 3 on four state-of-the-art EVs – the VW ID.3 Pro Performance, Porsche Taycan, Tesla Model 3 Standard Range Plus, and Tesla Model Y Long Range.

The curves show charging measurements at an early aging state and after utilization with more mileage covered. Evaluating the energy E_{calc} and capacity Q_{calc} between the specified voltage ranges given in Table 1 enables quantifying overall differences in the capacity/energy. Here, the SOH metrics are calculated with the EVs' nominal capacity and net energy, respectively, although these reference values were

most likely not determined by the exact proposed standard measurement. Thus, it is explicitly emphasized that a reference is an essential value for SOH comparability and must be available in the vehicle's registration documents with additional information available on how these values are determined. Note that the Porsche Taycan and Tesla Model Y measurements were conducted with different vehicles of the same model type and battery pack specification, demonstrating comparability between specimens.

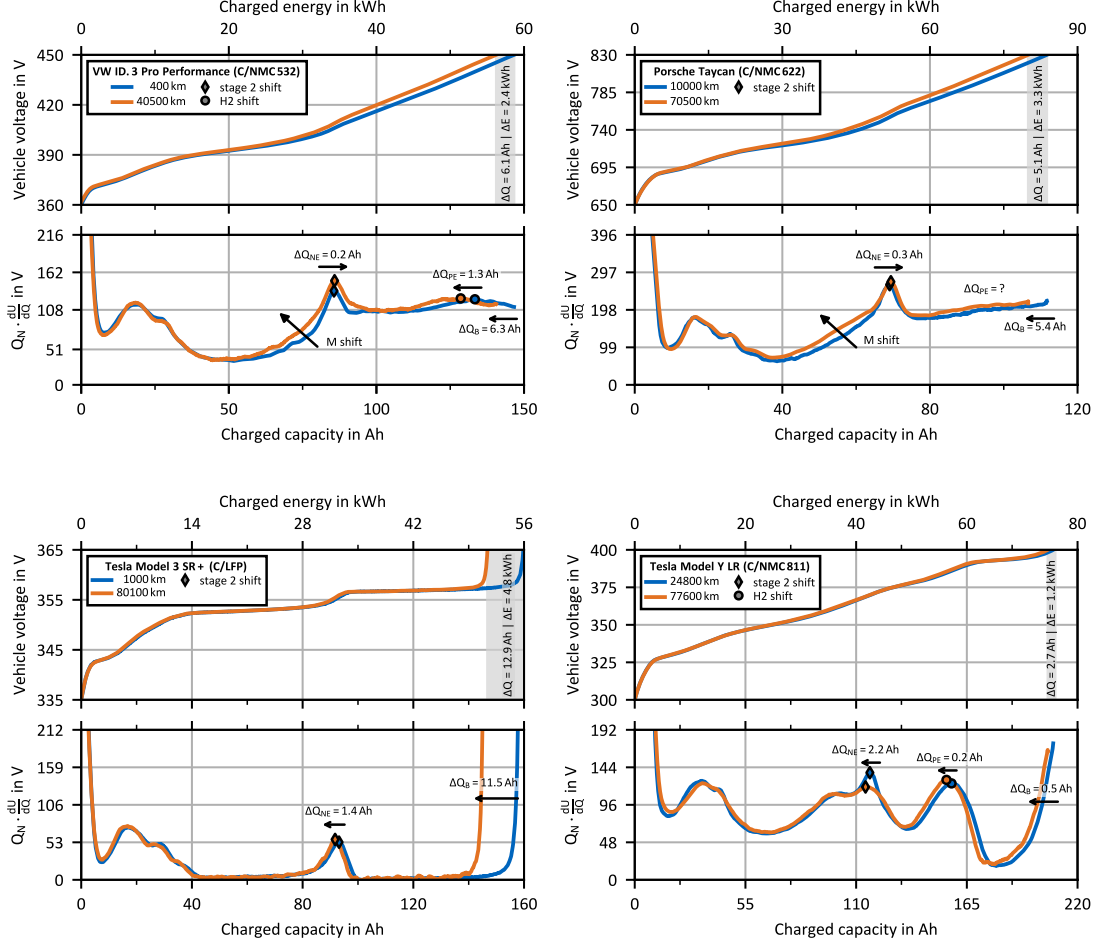


Fig. 3: Charging measurements of different vehicle models using the proposed standard charging measurement. a)-d) Voltage and DV curves of the VW ID.3, Porsche Taycan, Tesla Model 3, and Tesla Model Y. Insights from the DV curves show that LLI is the primary degradation mode of these battery packs.

Deeper insights into the electrochemical aging of the battery packs are given through DV analysis, where changes in the characteristic features Q_{PE} , Q_{NE} , and Q_B are labeled. LAM at the NE is identified for the Tesla Model 3 and Tesla Model Y. LAM at the PE can only be identified for the VW ID.3 and Tesla Model Y, as either there is no PE feature (e.g., for Tesla Model 3’s lithium iron phosphate (LFP) cells) or the feature is not unambiguously detectable (e.g., Porsche Taycan). For all vehicles, LLI, correlating with the change of the balancing feature Q_B , appears to be the predominant degradation mode at the time of the measurements and is mainly responsible for the loss of capacity/energy [39]. This aligns well with aging studies on the cell level under real-world conditions, where aging mechanisms binding lithium-ions, such as solid electrolyte interphase (SEI) formation, occur early in a battery’s service life, directly resulting in LLI [40]. The quantitative results for the measured capacities, energies, and degradation modes are summarized in Supplementary Table 1 in the supplementary information.

Discussion

The proposed standard charging procedure aims to provide an unambiguous and reproducible measurement for determining an EV battery pack’s SOH.

The most apparent disadvantage of the proposed standard measurement lies in its duration. However, the measurement time is essential to ensure an accurate calculation of the SOH, which is highly relevant to multiple stakeholders, given the battery pack’s critical role in vehicle utilization and asset valuation. Long idle periods – such as overnight parking – can be leveraged to conduct the measurement with minimal disruption. Moreover, the required measurement frequency remains low since battery aging generally occurs over several years. We therefore recommend performing the measurement once or twice per year. Exceptions apply in high usage cases, where more frequent measurements may be beneficial, or before the sale or purchase of a second-hand EV. Nevertheless, further research on the effects of higher charging powers on the standard measurement is encouraged to reduce the overall testing duration.

Furthermore, EV-specific peculiarities that influence the proposed procedure must be considered, which are discussed below.

For instance, measuring a fleet of the same vehicle model at similar mileages, shown in Figure 4a for five Cupra Borns, exhibits deviations in the pack voltages. Although cell-to-cell variations are of small order, they can become significant in the cell assembly [41]. Furthermore, individual onboard SOC estimations refer to different voltages, i.e., when all Cupras were completely charged, showing 100 % SOC in the user interface (UI), the voltages differed up to 5.4 V. Therefore, a fixed voltage window must be carefully defined to fit all vehicles of a model. This, however, affects the determination of the EV’s individual energy and capacity, as the fixed voltage ranges for the standard measurement crop the actual usable voltage window available in the vehicle. To compensate for this, each vehicle would need individual cut-off voltages, thereby inhibiting comparability. Differences in charging between fixed SOC and voltage boundaries, as well as the repeated measurements of one specimen, are given in Table 2, showcasing that fixing a voltage range is better suited for the comparability and reproducibility of the measurement results.

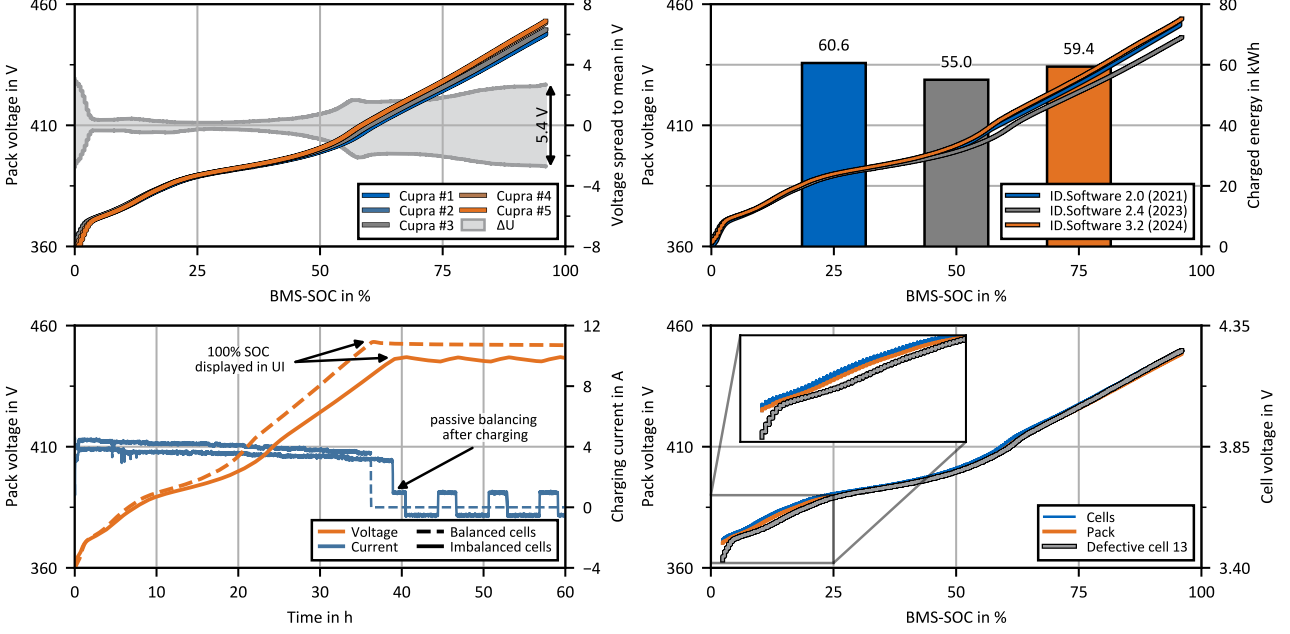


Fig. 4: Peculiarities of EVs and their influence on the proposed standard measurement. a) Measuring a fleet of identical vehicle models with comparable distance covered shows voltage differences so that the vehicle’s individual capacity/energy content is not reflected with a fixed voltage window. b) Software updates can change BMS settings, such as changing the voltage operation window as shown for annual measurements of the exact vehicle. c) Balancing occurs when cells within the pack have imbalanced SOC levels. Balancing phases after reaching 100 % UI-SOC are triggered by the BMS to realign the cells’ voltages. However, EVs in an unbalanced state can lead to inconsistent cut-off voltages. The consecutive measurements were conducted on the exact vehicle. d) Defective cells influence the battery system, e.g., cut-off conditions are met prematurely, and the measured capacity/energy is reduced. Note that for these VW vehicles, 96 % is the maximum BMS-SOC, which equals 100 % UI-SOC.

Likewise, interference of the BMS can hamper the standard measurement, e.g., software updates, possibly over-the-air, can change the voltage range of a battery pack, altering the usable operation window and capacity/energy retention, as shown in Figure 4b. Therefore, changes in the battery system must transparently be communicated to the vehicle owner so that the standard measurement and the reference for the SOH can be adjusted. Moreover, balancing through the BMS takes place to align the voltage levels of cells in the pack that have drifted due to (increasingly) differing aging levels, as seen in Figure 4c. Measuring a vehicle in an unbalanced state influences the standard measurement as the upper voltage limit might not be consistent, and features in DV curves can fade [42]. Therefore, the cells in the pack are ideally balanced prior to the measurement.

Also, a cell defect within the battery pack (Figure 4d) determines the usable capacity/energy, as cut-off voltages are met prematurely [43]. As a result, the defined voltage range may not be reachable on the pack level, and the SOH cannot be calculated with the proposed standard measurement. Nonetheless, if cell-level voltage data is available, targeted maintenance is possible to detect and locate faulty cells.

Regarding degradation assessment by DV analysis on the vehicle level, the previous examples have shown that degradation modes cannot always be determined, and limitations exist, e.g., BMS interference [20]. Also, it is unlikely for OEMs to publish voltage-capacity curves of pristine specimens for the evaluation of degradation modes. However, test facilities can establish databases for assessing aging between EVs of the same model type, as shown for the Porsche Taycan and Tesla Model Y.

Despite the limitations discussed, we are convinced that the proposed standard measurement based on charging is useful for the SOH determination for EVs' battery packs, and additional information from DV analysis adds value through deeper battery aging assessment. Thus an independent, external, and transparent battery diagnosis for EVs is enabled. Further, to maximize its effectiveness, we recommend that EV owners perform the proposed measurement at the beginning of the vehicle's life to establish a reference point for future evaluations, and enabling the possibility for individual aging analysis.

Nonetheless, due to the complexity of an EV's battery pack, a capacity- and energy-based SOH are merely two of many parameters necessary to fully characterize its multi-dimensional SOH [44]. For instance, we also encourage a standard measurement for the internal resistance (SOH_R) as it increases throughout an EV's lifetime and influences the usable SOC range, especially under high-power scenarios.

Hereby, the communications norms open charge point protocol (OCPP) 2.1 and ISO15118-20 can be useful, enabling bidirectional charging where more sophisticated battery diagnosis is possible through tailored (dis-)charging procedures, e.g., incorporating power pulses [45]. It is assumed that future EVs will comply with these norms and are capable of bidirectional charging.

Furthermore, data from vehicle sensors must be available for any onboard battery diagnostic method, e.g., through the OBD interface, without encryption in sufficient resolution, accuracy, precision, and sample rate, at least for the voltage, current, and SOC on the pack level. Additional access to further information, such as module temperatures and the cell voltage across each series connection, enables proactive and tailored maintenance, which is also encouraged. Thus, the OEMs must provide the required data, reference values, and the possibility of external battery diagnosis. For instance, Tesla's 'battery health' implementation is a step in the right direction but lacks transparency about the specific measurement procedure and how the SOH is calculated [46].

Ultimately, the legislator must ensure that independent battery diagnosis is possible, e.g., through the CEN/CENELEC standardization request M/579 aiming at "performance, safety and sustainability requirements for batteries", where our proposal can suit as a discussion basis [47].

Methods

The EVs under study are presented in [Section 1](#). Further, the measurement procedure ([Section 1](#)), vehicle data acquisition ([Section 1](#)), and postprocessing ([Section 1](#)) are explained in closer detail.

Vehicles under test

The vehicles under test are state-of-the-art EVs from VW, Cupra, Porsche and Tesla. The vehicles' battery specifications are summarized in [Table 1](#). All vehicles were purchased from a dealership or leased from non-OEM research partners to ensure unmodified mass-production specimens and an uninfluenced examination.

Seven Volkswagen Group vehicles sharing the same battery pack with NMC532/graphite cells were tested: Five Cupra Borns with similar mileages (12 700-17 700 km) and two VW ID.3s. Both first-generation VW ID.3s were purchased in 2020. The vehicle analyzed for aging was comprehensively investigated through teardown analysis by Wassiliadis et al. [\[6\]](#). This specimen was subject to multiple measurements between mileages of 400 km and 40 500 km at different software releases and balancing states and was previously analyzed by DV analysis at lower mileages [\[20\]](#). The second VW ID.3 has a defective cell limiting the overall battery pack performance.

The 2020 Tesla Model 3 Standard Range Plus is equipped with prismatic LFP/graphite cells that have been comprehensively investigated at the cell level [\[48\]](#) and vehicle level [\[26\]](#). The vehicle was measured at mileages 1000 km and 80 100 km and was previously analyzed by DV analysis at lower mileages [\[20\]](#).

Two 2022 Porsche Taycans from different sources were measured at mileages of 10 000 km and 70 500 km. Both vehicles share the same battery pack with NMC622/graphite cells. Also two Tesla Model Y Long Range vehicles (manufactured in 2022 and 2024) with mileages of 77 600 km and 24 800 km were measured. Ank et al. [\[49\]](#) investigated the NMC 811/graphite chemistry used by both vehicles. These measurements show that aging assessment through the proposed standard measurement is comparable within vehicle models.

Measurement procedure

A battery cell's remaining capacity/energy is typically determined during reoccurring check-ups from controlled (dis-)charging cycles between fixed boundary constraints [\[50\]](#). This general procedure is transferred onto the vehicle level through a controlled charging cycle adapted to the vehicles' usage window, similar to Wassiliadis et al. [\[6\]](#). Note that the SOC displayed in the UI differs from the BMS-SOC, possibly to preserve energy buffers. Here, only the BMS-SOC is considered.

The vehicles are fully discharged to 0 % SOC before the measurement, whereby the last few percent are drained using auxiliary units. After the discharging procedure, the vehicles were set to rest for approx. 30 min for further overpotentials to settle before the charging session is triggered by connecting the vehicle to the AC (IEC 61851 mode) charging device Juice Booster 2 (Juice Technology, Switzerland). The charging device can supply charging powers between 1.4 kW and 22 kW depending on the connected socket (single/triple phase). A quasi-stationary measurement is sought by preferring

low charging powers to reduce the effects of overpotentials and inhomogeneity in the NE [51]. Therefore, the charging power is set to yield at least a 30 h charging session calculated by the vehicles' net energy content. Other authors found that a 15 h charging session is sufficient and does not mitigate the SOH calculation or aging assessment [35]. The vehicles are exclusively charged inside a workshop at an ambient temperature of 20 °C until the BMS terminates the charging session. The capacity and energy are calculated between fixed voltage ranges, given in Table 1 defined for each EV model.

Data acquisition

The measurement procedure relies on onboard sensor data of the vehicles under test, which is recorded using different methods depending on the manufacturer. The most relevant high voltage (HV) battery pack level signals are the voltage, current, and BMS/UI-SOC. The cell voltages across each serial connection and temperature data are also sampled when available. The data is recorded with the precision of the built-in sensors that have sufficient data quality for further processing [20].

The entire CAN bus communication is recorded for the Tesla vehicles via a CAN interface with the recording tool Busmaster. The data is converted into physical and human-readable quantities by a publicly available .dbc file from GitHub. The correctness of the conversion schemes is asserted by comparison to data from a commercially available vehicle diagnostic device, which is unsuitable for logging over a long period. The sample rate is 100 Hz for the pack current, voltage, and SOC and 0.5 Hz for the cell voltages. The resolution of the digitized signals can be estimated from the sampled data as 0.1 V for the voltages, 0.1 A for the current, and 0.1 % for the SOC.

Data from the VW group vehicles is queried by unified diagnostic services (UDS) sent through the OBD-II diagnostic interface and converted with a custom UDS decoder tool. Each request addresses a unique identifier (ID) reverse-engineered by reproducing the traffic from a commercially available vehicle diagnostic device. An in-depth description of the data acquisition is given by Merkle et al. [52]. During the measurement, the individual values are requested at 1 Hz. However, the gateway board, responsible for handling requests, responds to requests depending on the available bandwidth. In practice, a sample is logged in a frequency between 0.1 Hz and 1 Hz. The resolution of the digitized signals can be estimated from the sampled data as 0.25 V for the voltages, 0.1 A for the current, and 0.40 % for the SOC.

Data postprocessing

The long-format data traces are subsequently synchronized onto a single time vector by linear interpolation and cropped to fit the voltage range specified in Table 1. The data is filtered by a mean filter in the forward direction with a window size of 1 % of data points to generalize between different vector lengths. The capacity Q_{calc} and E_{calc} are calculated by Equation 2 and Equation 3, respectively.

The DV curve is calculated from the derivatives of the pack voltage and capacity signals by

$$DV = \frac{dU/dt}{dQ/dt} \approx \frac{\Delta U}{\Delta Q}. \quad (6)$$

For practical applications, the DV curve is calculated by forward difference schemes [53]. Furthermore, the DV curve is normalized by the nominal capacity Q_N given in Table 1, through which the data is scaled in y-direction around the number of series-connected cells in the battery pack, enhancing the comparability between battery systems with different capacities. Care must be taken when applying filtering methods, as these can alter features of interest [54].

Declarations

Data availability. We want to give any researcher access to our data without any limits. The data of all measurements can be found at [mediaTUM](#). Press login at top left of page. Access: reviewer-access-12, password: QjvP@Lv-ea848!22hUkPM

Code availability. The code for processing the data and generating the figures is available at [FTM Github](#).

Acknowledgements. This research received funding from the Bavarian Ministry of Economic Affairs, Regional Development, and Energy within the project 'charge.COM' under the grant number DIK-0262/02. Furthermore, this work was partly funded by the German Federal Ministry for Economic Affairs and Climate Action (BMWK) within the project 'ultraBatt' under the grant number 01MV21015D and the German Federal Ministry of Education and Research (BMBF) within the project 'BALd' under grant number 03XP0320B. The funders played no role in the study design, data collection, analysis, and interpretation of data or the writing of this manuscript. We also thank TUM.Battery for promoting battery research by providing an interdisciplinary network of experts.

Author contributions. P.B. initiated the idea, conducted measurements, and wrote the paper. M.S. conducted measurements, contributed to the standard measurement, and interpretation of the results. P.R. conducted measurements, contributed to the methods and discussion. K.A.G., J.S., and C.G. supported the measurements, analyzed the data, and addressed customer relevance. M.L. contributed to the concept and supervised the research. All authors discussed the results, wrote sections, and revised the paper thoroughly and critically.

Conflict of interest/Competing interests. The authors declare that they have no known competing financial interests or personal relationships that could have appeared to influence the work reported in this paper.

References

- [1] Woody, M., Keoleian, G. A. & Vaishnav, P. Decarbonization potential of electrifying 50% of u.s. light-duty vehicle sales by 2030. *Nature communications* **14**, 7077 (2023).
- [2] Dühnen, S. *et al.* Toward Green Battery Cells: Perspective on Materials and Technologies. *Small Methods* **4** (2020).
- [3] John Kiser and Graham Gordon. Why electric vehicle interest is stagnating at the worst possible time. *Ipsos* (2023).
- [4] Edge, J. S. *et al.* Lithium ion battery degradation: what you need to know. *Physical chemistry chemical physics : PCCP* **23**, 8200–8221 (2021).
- [5] Demirci, O., Taskin, S., Schaltz, E. & Acar Demirci, B. Review of battery state estimation methods for electric vehicles-part ii: Soh estimation. *Journal of Energy Storage* **96**, 112703 (2024).
- [6] Wassiliadis, N. *et al.* Quantifying the state of the art of electric powertrains in battery electric vehicles: Range, efficiency, and lifetime from component to system level of the Volkswagen ID.3. *eTransportation* **12**, 100167 (2022).
- [7] Dubarry, M. & Baure, G. Perspective on Commercial Li-ion Battery Testing, Best Practices for Simple and Effective Protocols. *Electronics* **9**, 152 (2020).
- [8] Hu, X., Le Xu, Lin, X. & Pecht, M. Battery lifetime prognostics. *Joule* **4**, 310–346 (2020).
- [9] Harper, G. *et al.* Recycling lithium-ion batteries from electric vehicles. *Nature* **575**, 75–86 (2019).
- [10] Sulzer, V. *et al.* The challenge and opportunity of battery lifetime prediction from field data. *Joule* **5**, 1934–1955 (2021).
- [11] Schaltz, E., Stroe, D.-I., Norregaard, K., Ingvarlsen, L. S. & Christensen, A. Incremental Capacity Analysis Applied on Electric Vehicles for Battery State-of-Health Estimation. *IEEE Transactions on Industry Applications* **57**, 1810–1817 (2021).
- [12] Rufino Júnior, C. A. *et al.* Towards to battery digital passport: Reviewing regulations and standards for second-life batteries. *Batteries* **10**, 115 (2024).
- [13] European Parliament and Council. [Regulation \(EU\) 2023/1542 of the European Parliament and of the Council of 12 July 2023 concerning batteries and waste batteries](#) (2023). Visited on 26.05.2025.

- [14] Battery Pass consortium. [Battery Passport Content Guidance](#) (2023). Visited on 26.05.2025.
- [15] United Nations Economic and Social Council (UNECE). [United Nations Global Technical Regulation on In-vehicle Battery Durability for Electrified Vehicles](#) (2024). Visited on 26.05.2025.
- [16] European Parliament and Council. [Regulation \(EU\) 2024/1257 on type-approval of motor vehicles and engines and of systems, components and separate technical units intended for such vehicles, with respect to their emissions and battery durability \(Euro 7\)](#) (2024). Visited on 26.05.2025.
- [17] International Organization for Standardization. [12405:2018: Electrically propelled road vehicles - Test specification for lithium-ion traction battery packs and systems - Part 4: Performance testing](#) (2018). Visited on 26.05.2025.
- [18] Yao, L. *et al.* A review of lithium-ion battery state of health estimation and prediction methods. *World Electric Vehicle Journal* **12**, 113 (2021).
- [19] Gutwald, B., Lehmann, R., Barth, M., Reichenstein, T. & Franke, J. Bi-directional dc charging stations for evs on renewable-powered lvdc grids: Design, sizing, control and testing (2024).
- [20] Bilfinger, P. *et al.* Battery pack diagnostics for electric vehicles: Transfer of differential voltage and incremental capacity analysis from cell to vehicle level. *eTransportation* **22**, 100356 (2024).
- [21] Agency, I. E. [Global EV Outlook 2024: Moving Towards Increased Affordability](#) (2024). Visited on 26.05.2025.
- [22] Barai, A. *et al.* A comparison of methodologies for the non-invasive characterisation of commercial Li-ion cells. *Progress in Energy and Combustion Science* **72**, 1–31 (2019).
- [23] Kim, J., Park, S., Hwang, S. & Yoon, W.-S. Principles and applications of galvanostatic intermittent titration technique for lithium-ion batteries. *Journal of Electrochemical Science and Technology* **13**, 19–31 (2022).
- [24] [Electric vehicle model statistics — European Alternative Fuels Observatory](#) (16.12.2024). Visited on 26.05.2025.
- [25] Danko, M., Adamec, J., Taraba, M. & Drgona, P. Overview of batteries State of Charge estimation methods. *Transportation Research Procedia* **40**, 186–192 (2019).
- [26] Rosenberger, N. *et al.* Quantifying the State of the Art of Electric Powertrains in Battery Electric Vehicles: Comprehensive Analysis of the Tesla Model 3 on the

Vehicle Level. *World Electric Vehicle Journal* **15**, 268 (2024).

- [27] Qi, Q. *et al.* Battery pack capacity estimation for electric vehicles based on enhanced machine learning and field data. *Journal of Energy Chemistry* **92**, 605–618 (2024).
- [28] Farmann, A., Waag, W., Marongiu, A. & Sauer, D. U. Critical review of on-board capacity estimation techniques for lithium-ion batteries in electric and hybrid electric vehicles. *Journal of Power Sources* **281**, 114–130 (2015).
- [29] Rashid, M. & Gupta, A. Effect of relaxation periods over cycling performance of a li-ion battery. *Journal of The Electrochemical Society* **162**, A3145–A3153 (2015).
- [30] Fernando, A., Kuipers, M., Angenendt, G., Kairies, K.-P. & Dubarry, M. Benchmark dataset for the study of the relaxation of commercial nmc-811 and lfp cells. *Cell Reports Physical Science* **5**, 101754 (2024).
- [31] Waldmann, T., Wilka, M., Kasper, M., Fleischhammer, M. & Wohlfahrt-Mehrens, M. Temperature dependent ageing mechanisms in lithium-ion batteries – a post-mortem study. *Journal of Power Sources* **262**, 129–135 (2014).
- [32] Schaltz, E., Stroe, D.-I., Norregaard, K., Kofod, L. & Christensen, A. *Incremental Capacity Analysis for Electric Vehicle Battery State-of-Health Estimation* (IEEE, Piscataway, NJ, 2019).
- [33] von Bülow, F., Wassermann, M. & Meisen, T. State of health forecasting of lithium-ion batteries operated in a battery electric vehicle fleet. *Journal of Energy Storage* **72**, 108271 (2023).
- [34] Jossen, A. & Weydanz, W. *Moderne Akkumulatoren richtig einsetzen* 2. überarbeitete auflage edn (MatrixMedia Verlag, Göttingen, 2021). isbn: 978-3-946891-18-5 .
- [35] Schmitt, J., Rehm, M., Karger, A. & Jossen, A. Capacity and degradation mode estimation for lithium-ion batteries based on partial charging curves at different current rates. *Journal of Energy Storage* **59**, 106517 (2023).
- [36] Fly, A. & Chen, R. Rate dependency of incremental capacity analysis (dQ/dV) as a diagnostic tool for lithium-ion batteries. *Journal of Energy Storage* **29**, 101329 (2020).
- [37] Bloom, I. *et al.* Differential voltage analyses of high-power lithium-ion cells – 1. Technique and application. *Journal of Power Sources* **139**, 295–303 (2005).
- [38] Wildfeuer, L. *et al.* Experimental degradation study of a commercial lithium-ion battery. *Journal of Power Sources* **560**, 232498 (2023).

- [39] Schreiber, M. *et al.* Understanding lithium-ion battery degradation in vehicle applications: Insights from realistic and accelerated aging tests using volkswagen id.3 pouch cells. *Journal of Energy Storage* **112**, 115357 (2025).
- [40] Geslin, A. *et al.* Dynamic cycling enhances battery lifetime. *Nature Energy* (2024).
- [41] Rumpf, K., Naumann, M. & Jossen, A. Experimental investigation of parametric cell-to-cell variation and correlation based on 1100 commercial lithium-ion cells. *Journal of Energy Storage* **14**, 224–243 (2017).
- [42] Reiter, A., Lehner, S., Bohlen, O. & Sauer, D. U. Electrical cell-to-cell variations within large-scale battery systems — A novel characterization and modeling approach. *Journal of Energy Storage* **57**, 106152 (2023).
- [43] Baumann, M., Wildfeuer, L., Rohr, S. & Lienkamp, M. Parameter variations within Li-Ion battery packs – Theoretical investigations and experimental quantification. *Journal of Energy Storage* **18**, 295–307 (2018).
- [44] von Bülow, F., Heinrich, F. & Paxton, W. A. The future of battery data and the state of health of lithium-ion batteries in automotive applications. *Communications engineering* **3**, 173 (2024).
- [45] Willrett, U. Innovative charging functions using iso 15118-20 (2023). isbn:978-3-658-42047-5 .
- [46] Tesla. [Tesla’s High Voltage Battery Health](#). Visited on 26.05.2025.
- [47] European Commission. [C\(2021\)8614 – Standardisation request M/579](#) (2024). Visited on 26.05.2025.
- [48] Stock, S. *et al.* Cell teardown and characterization of an automotive prismatic LFP battery. *Electrochimica Acta* **471**, 143341 (2023).
- [49] Ank, M. *et al.* Lithium-Ion Cells in Automotive Applications: Tesla 4680 Cylindrical Cell Teardown and Characterization. *Journal of The Electrochemical Society* **170**, 120536 (2023).
- [50] Severson, K. A. *et al.* Data-driven prediction of battery cycle life before capacity degradation. *Nature Energy* **4**, 383–391 (2019).
- [51] Lewerenz, M. & Sauer, D. U. Evaluation of cyclic aging tests of prismatic automotive linimncoo₂-graphite cells considering influence of homogeneity and anode overhang. *Journal of Energy Storage* **18**, 421–434 (2018).
- [52] Merkle, L., Pöthig, M. & Schmid, F. Estimate E-Golf Battery State Using Diagnostic Data and a Digital Twin. *Batteries* **7**, 15 (2021).

- [53] Smith, A. J. & Dahn, J. R. Delta Differential Capacity Analysis. *Journal of The Electrochemical Society* **159**, 290–293 (2012).
- [54] Dubarry, M. & Anseán, D. Best practices for incremental capacity analysis. *Frontiers in Energy Research* **10** (2022).
- [55] Keil, P. & Jossen, A. Calendar Aging of NCA Lithium-Ion Batteries Investigated by Differential Voltage Analysis and Coulomb Tracking (2017).
- [56] F. J. Günter & N. Wassiliadis. State of the Art of Lithium-Ion Pouch Cells in Automotive Applications: Cell Teardown and Characterization. *Journal of The Electrochemical Society* (2022).

Table 1: Overview of vehicle specifications from the vehicles under study.

Attribute	Unit	VW ID.3 Pro Performance ^e	Porsche Taycan	Tesla Model 3 SR+ (LFP)	Tesla Model Y LR (NMC)
Gross energy ^a	kW h	62	93.4	55	77
Net energy ^b	kW h	58	82.3	52.5	75
Nom. capacity	A h	145 ^d	112 ^d	161.5 ^c	211.6 ^c
Voltage range ^d	V	360 – 450	650 – 830	335 – 365	300 – 400
Serial cells ^b	-	108	198 ^c	106	96
Parallel cells ^b	-	2	2 ^c	1	46
Cell format ^b	-	pouch	pouch ^c	prismatic	cylindrical
Chemistry ^c	-	C/NMC532	C/NMC622	C/LFP	C/NMC811

^a Vehicle registration documents

^b EV Database: [Volkswagen ID.3 Pro Performance](#), [Porsche Taycan](#), [Tesla Model 3 Standard Range Plus](#), [Tesla Model Y Long Range](#)

^c Literature: VW [56], [Porsche Taycan](#), Tesla Model 3 [48], Tesla Model Y [49]

^d Measurement data

^e Same specifications for Cupra Born

Table 2: Comparison of charged energy during the standard measurement across five Cupras with fixed SOC and voltage windows. Cupra 213 was measured three times to assess reproducibility.

Measuring window		0-100 % SOC		370-445 V ^b	
Vehicle ^a	Mileage in km	Voltage range in V	Charged energy in kW h	SOC range in %	Charged energy in kW h
Cupra 397	12750	359.0 – 447.6	56.5	3.2 – 93.6	53.3
Cupra 349	12600	363.0 – 449.3	57.8	2.4 – 92.4	53.9
Cupra 288	13250	361.8 – 449.3	57.7	2.4 – 92.0	53.7
Cupra 204	17700	358.8 – 452.2	58.7	3.2 – 89.6	52.7
Cupra 213 (I)	15300	357.2 – 453.0	60.5	3.2 – 89.2	53.8
Cupra 213 (II)	15300	359.0 – 453.0	60.5	3.2 – 89.2	53.9
Cupra 213 (III)	15300	363.5 – 452.6	59.9	2.4 – 89.2	54.0

^a The number refers to the vehicle’s licence plate.

^b The voltage range was chosen to fit all specimens.